

Supporting Information

Two-step preparation of cyano-functionalized linkage-hybrid covalent organic frameworks for efficient H₂O₂ photosynthesis in air

Han Ren,^{†a} Yuxuan Liu,^{†a} Zhecheng Huang,^a Liecheng Guo,^a and Feng Luo^{a*}

East China University of Technology, Nanchang 330013, China

E-mail: ecitluofeng@163.com

EXPERIMENTAL SECTION

1. Materials and general methods

The raw materials for synthesizing COF and these organic solvents (99%) were purchased from Aladdin Bio chemical Technology Co., Ltd. All these reagents were used as received without further purification. X-ray powder diffraction was collected by a Bruker AXSD8 Discover or D8 ADVANCE powder diffractometer. The simulated powder patterns were calculated by Mercury 1.4. Infrared Spectra (IR) was measured by a Bruker VERTEX70 spectrometer in the 700–3600 cm^{-1} region. The gas adsorption isotherms were collected on a Belsorp-max. Ultrahigh-purity-grade (>99.999%) N_2 gases were used during the adsorption measurement. X-ray photoelectron spectrum (XPS) were collected by Thermo Scientific ESCALAB 250 Xi spectrometer. Scanning electron microscopy (SEM) images were recorded on a Hitachi SU 8100 Scanning Electron Microscope. Photoelectrochemical experiments measurements were performed on a CHI760 workstation. UV–vis spectroscopy results were recorded in diffuse reflectance (DR) mode at room temperature on a SHIMADZU UV-2700 spectrophotometer equipped with an integrating sphere attachment. Solid-state NMR experiments were performed on Varian Infinityplus 300 solid-state NMR spectrometer (300 MHz). The photoluminescence decay profiles were measured by using time-correlated single photon counting (TCSPC) mode on a Picosecond Lifetime Fluorescence Spectrometer (QUANTAUROS-TAU C11367-11). Electron spin resonance (ESR) was used to investigate the reactive species, which was recorded using a Bruker A300 spectrometer. Specifically, the 5,5-dimethyl-1-pyrroline-N-oxide (DMPO) was used to trap the superoxide radical ($\cdot\text{O}_2^-$).

2. Synthesis of BTAC

The BTAC is synthesized using benzene-1,3,5-tricarbaldehyde (BT, 0.5 mmol) and 2-(4-aminophenyl) acetonitrile (AC, 1.5 mmol) in a mixture of water (10 mL), ethanol (10 mL) and sodium hydroxide (500 mg), which is stirred and heated at 85 °C for 2 hours. The precipitate is collected by filtration, washed with NaOH, $\text{C}_2\text{H}_5\text{OH}$

and water for many times, and finally dried at 80 °C under vacuum overnight to give BTAC in a yield of 46%.

3. Synthesis of ECUT-COF-95

The ECUT-COF-95 is synthesized using 1,3, 5-triformyl-phloroglucinol (TP) (21 mg, 0.1 mmol), BTAC (56 mg, 0.1 mmol) in a mixture of o-dichlorobenzene (2 mL), 1-butanol (2 mL) and acetic acid (6 M, 0.4 mL), which is degassed in a Pyrex tube (25 mL) by three freeze-pump-thaw cycles. The tube is sealed and heated at 120 °C for 3 days. The precipitate is collected by filtration, washed with DMF and methanol for many times, and finally dried at 80 °C under vacuum overnight to give ECUT-COF-95 in a yield of 65%.

4. Synthesis of ECUT-COF-96

The ECUT-COF-96 is synthesized using BT (16 mg, 0.1 mmol), BTAC (56 mg, 0.1 mmol) in a mixture of o-dichlorobenzene (2 mL), 1-butanol (2 mL) and acetic acid (6 M, 0.4 mL), which is degassed in a Pyrex tube (25 mL) by three freeze-pump-thaw cycles. The tube is sealed and heated at 120 °C for 3 days. The precipitate is collected by filtration, washed with DMF and methanol many times, and finally dried at 80 °C under vacuum overnight to give ECUT-COF-96 in a yield of 57%.

5. Photosynthesis of hydrogen peroxide

5 mg of catalyst, 50 mL of deionized water (or 48 mL of water and 2 mL of active species trapping agent). The mixture was stirred continuously under a xenon lamp for various time. The solution was filtered through an organic filter membrane and the content of H₂O₂ was determined by UV-Vis spectrophotometry as follows. Typically, 1 mL testing solution, 1 mL potassium hydrogen phthalate (0.1 mol/L), and 1 mL potassium iodide (0.4 mol/L) were mixed and added into a 10 mL volumetric flask, and palced for one hour. A maximum absorption wavelength of 350 nm was used to measure the concentration of hydrogen peroxide.

6. Apparent quantum yield (AQY)

The measurement of apparent quantum yield (AQY) is similarly carried out according to literature (*Nat. Catal.* 2024, 7, 195-206; *Angew. Chem. Int. Ed.* 2024, 63, e202400999). The apparent quantum yield (AQY) is calculated by measuring H₂O₂ photosynthesis of ECUT-COF-95 and ECUT-COF-96 under 400 nm monochromatic light irradiation. The light intensity is measured by a digital optical power and energy meter of PROVA-1010. The light intensity is maintained about 0.1 W/m². The photocatalytic reaction is carried out in deionized water (50 mL) with photocatalyst (5 mg). The active area of the reactor is approximately 3 cm². AQY is then calculated by the following formula:

$$AQY (\%) = \frac{[GH_2O_2 \text{ produced (mol)}] \times 2}{\text{photons entered the reactor (mol)}} \times 100\%$$

$$= \frac{[N_a \times h \times c][GH_2O_2 \text{ produced (mol)}] \times 2}{t \times S \times I \times \lambda} \times 100\%$$

where N_a is the Avogadro's constant (6.022×10^{23}), h is the Planck constant (6.626×10^{-34}), c is the speed of light (3×10^8), S is the irradiation area (cm²), I is the intensity of light irradiation (W/m²), t is the irradiation time (3600 s) and λ is the irradiation wavelength (4×10^{-7} m).

7. Photocatalytic experiments in different environments

The efficient H₂O₂ production of them in open air further prompts us to explore the application of them in real-time H₂O₂ production from various waters. First, we find that both of them are efficient for H₂O₂ production in acidic and basic water with pH=1 and 9, showing a H₂O₂ production rate of respectively 2318 and 1845 $\mu\text{mol h}^{-1} \text{g}^{-1}$ for ECUT-COF-95 and 2398 and 2522 $\mu\text{mol h}^{-1} \text{g}^{-1}$ for ECUT-COF-96 (Fig. S12). This value is comparable with that observed in pure water for both of them. Next, we investigate the H₂O₂ production upon them in the common water sources around us such as tap water, river water, lake water, and seawater. The results are shown in Fig. S13. Clearly, both of COFs are efficient for H₂O₂ production in these medium with the H₂O₂ production rate of $>1300 \mu\text{mol h}^{-1} \text{g}^{-1}$ for ECUT-COF-95 and $>1500 \mu\text{mol h}^{-1} \text{g}^{-1}$ for ECUT-COF-96. The above results strongly confirm the superior potential of the two COFs for the real-time H₂O₂ production in various water environments.

8. Rhodamine B degradation assay

In industry, one important application of H₂O₂ is the degradation of organic

dyes. Subsequently, in light of the real-time H₂O₂ production performance in both of COFs in open air and various water environments, we then carried out the investigation of H₂O₂ photosynthesis upon both of COFs coupling with in-situ degradation of Rhodamine B from a 10 mg/L Rhodamine B solution. Clearly, both of them are efficient for the photocatalytic degradation of Rhodamine B in open air. For ECUT-COF-96, it can enable a 100% removal rate within 30 minutes, while ECUT-COF-95 needs 60 minutes to perform the same outcome (Fig. S14). The results strongly suggest their superior application in water cleanup.

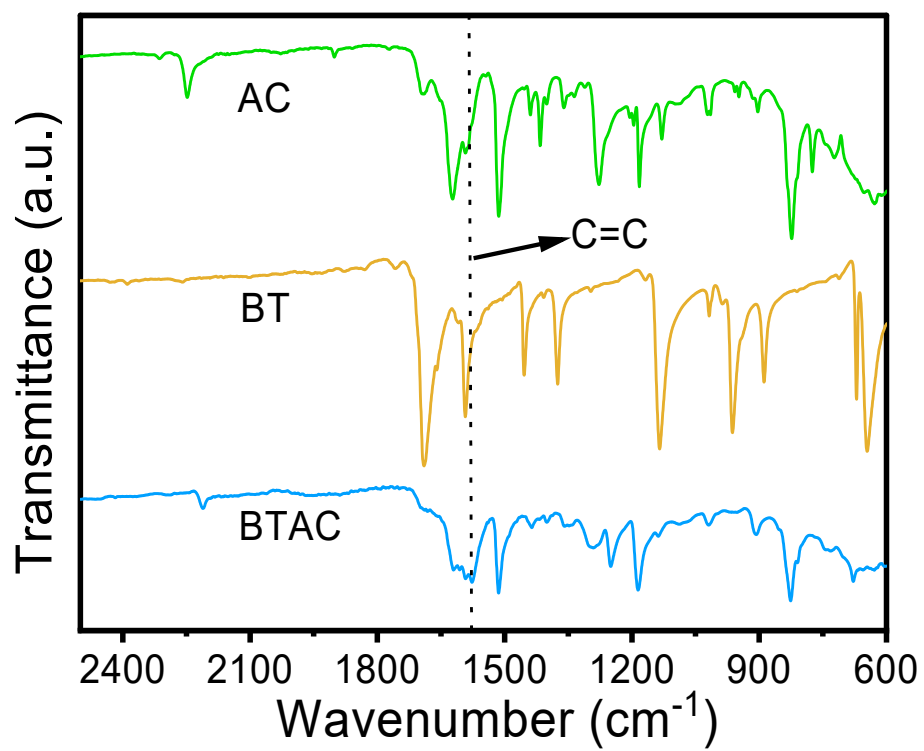


Fig. S1 The IR of BTAC.

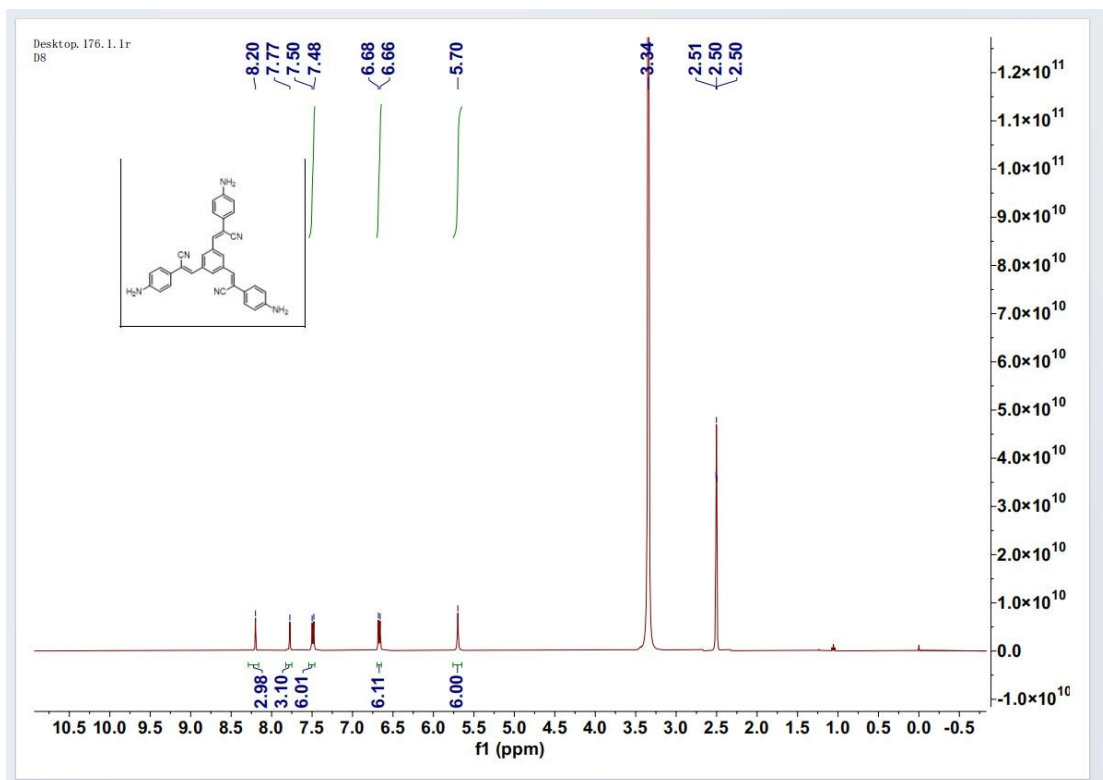


Fig. S2 The ^1H NMR of BTAC.

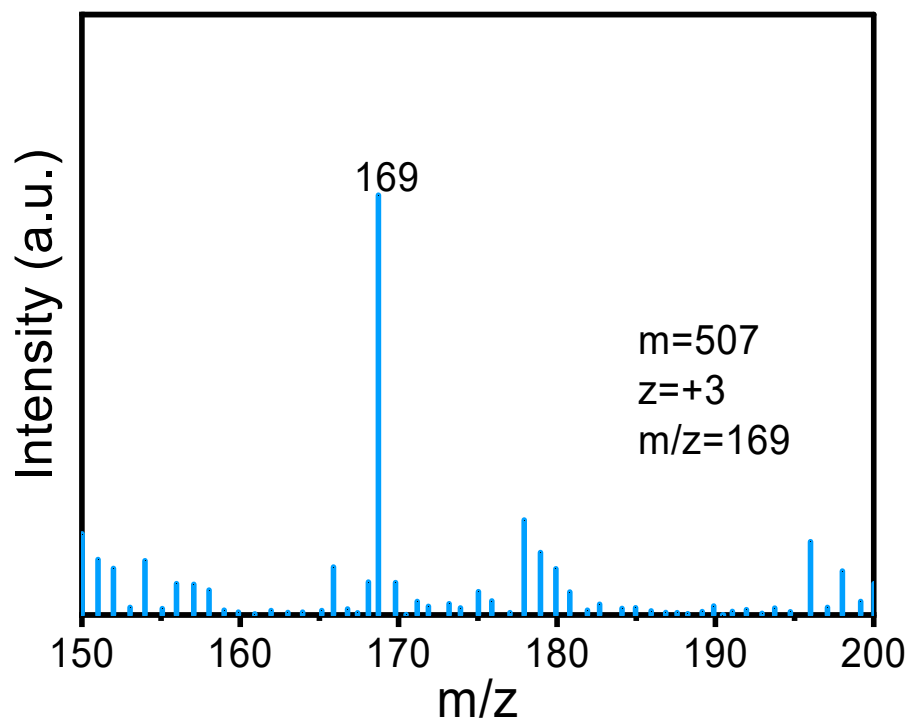


Fig. S3 MS of BTAC.

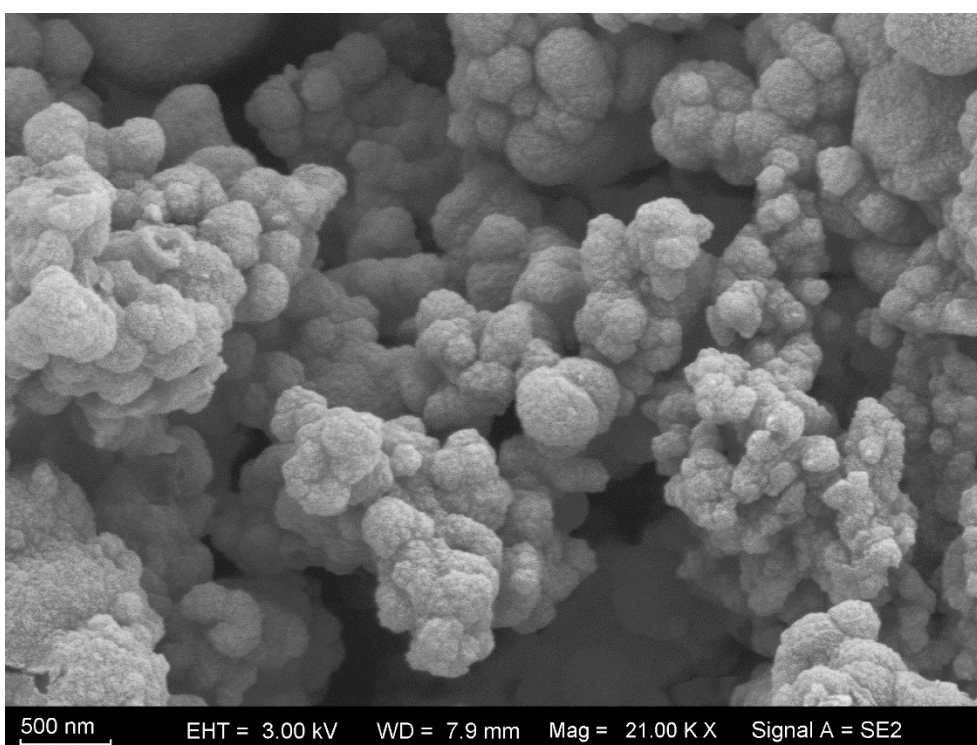
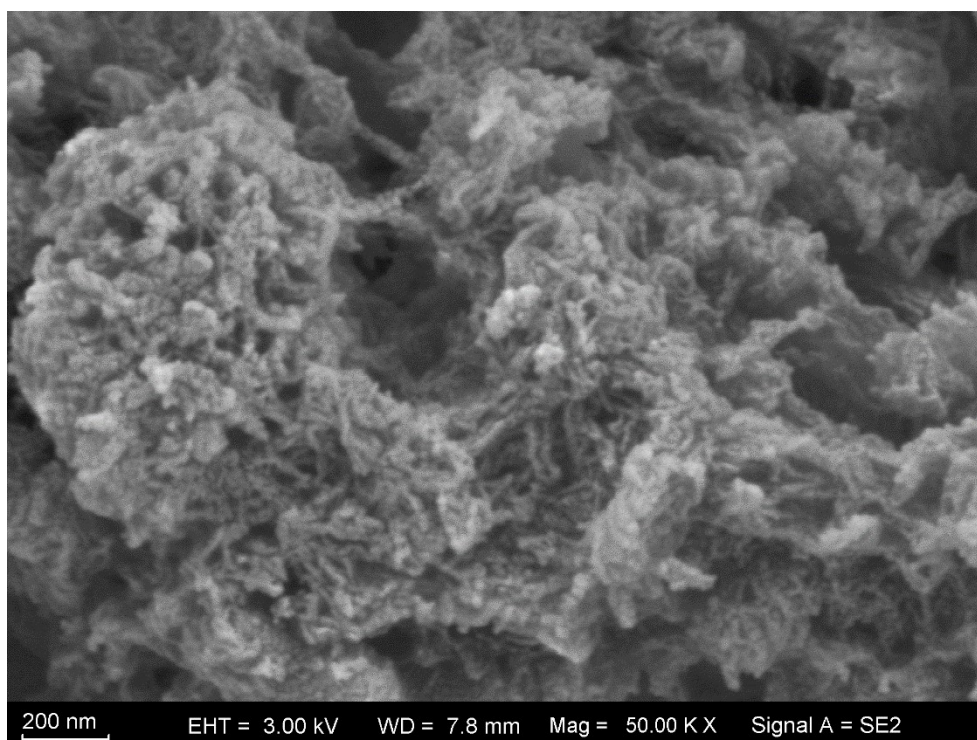


Fig. S4 SEM image of ECUT-COF-95 (above) and ECUT-COF-96 (below).

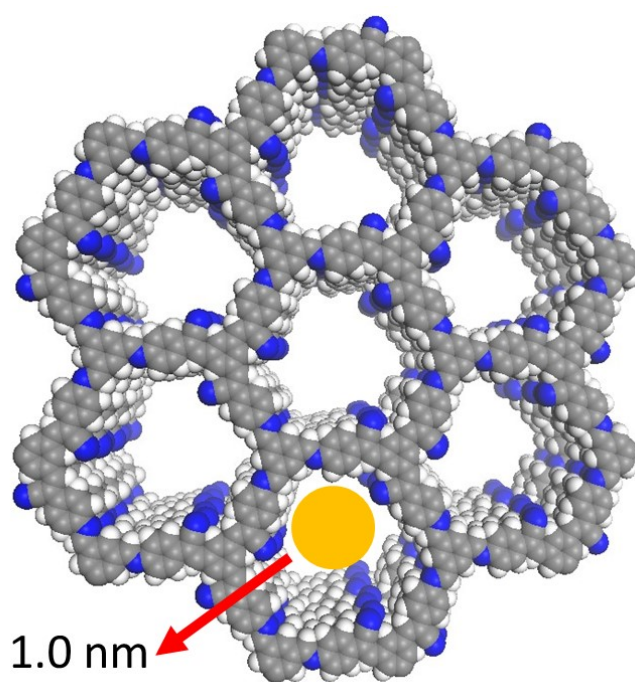
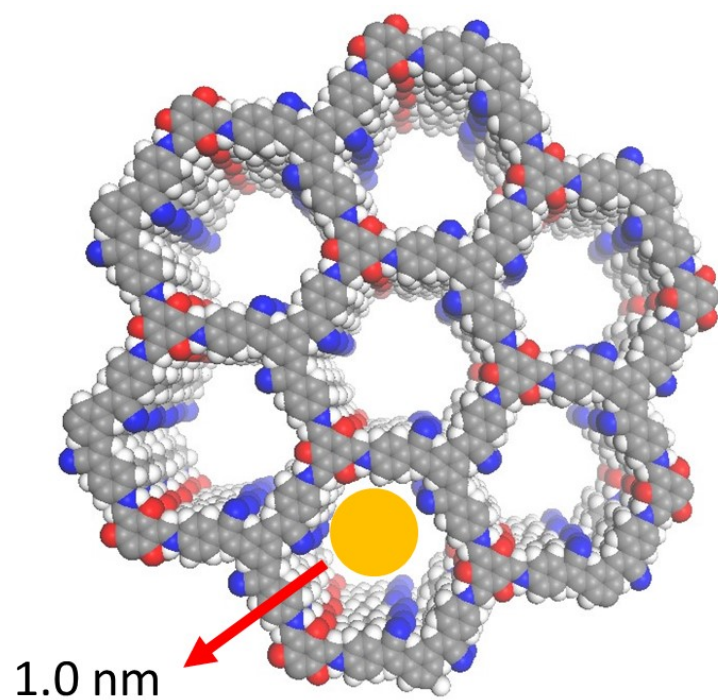


Fig. S5 AA stacking structural representations of ECUT-COF-95 (above) and ECUT-COF-96 (below).

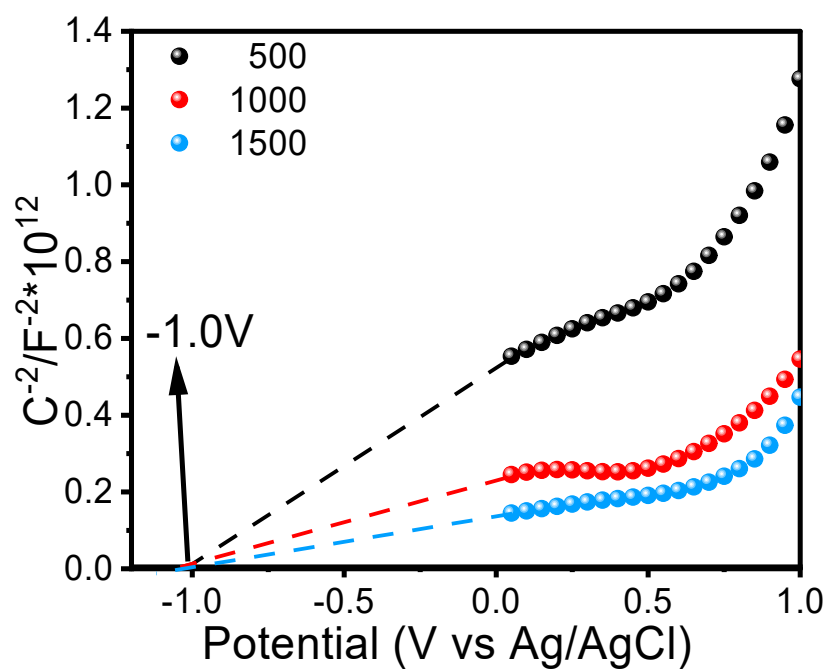
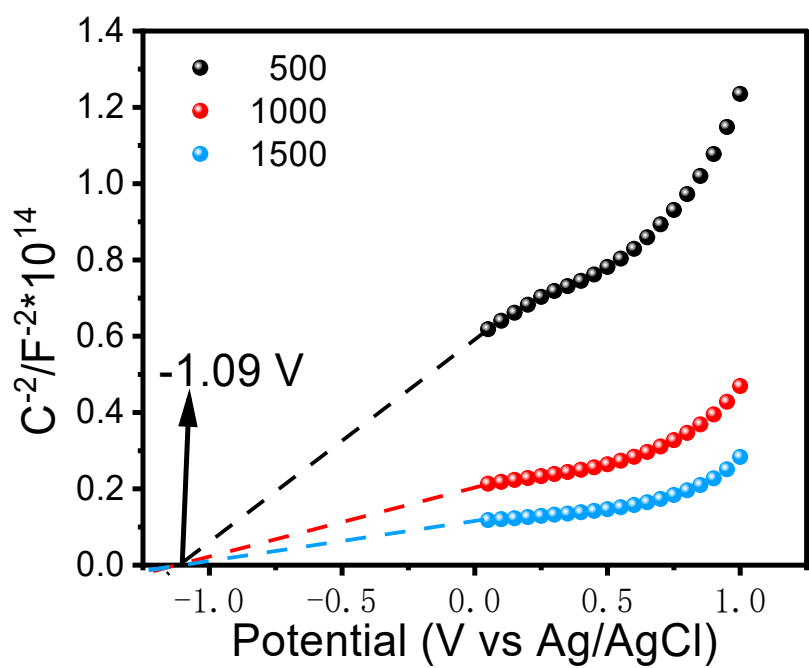


Fig. S6 Mott-Schottky plots of ECUT-MCOF-95 (above) and ECUT-MCOF-96 (below).

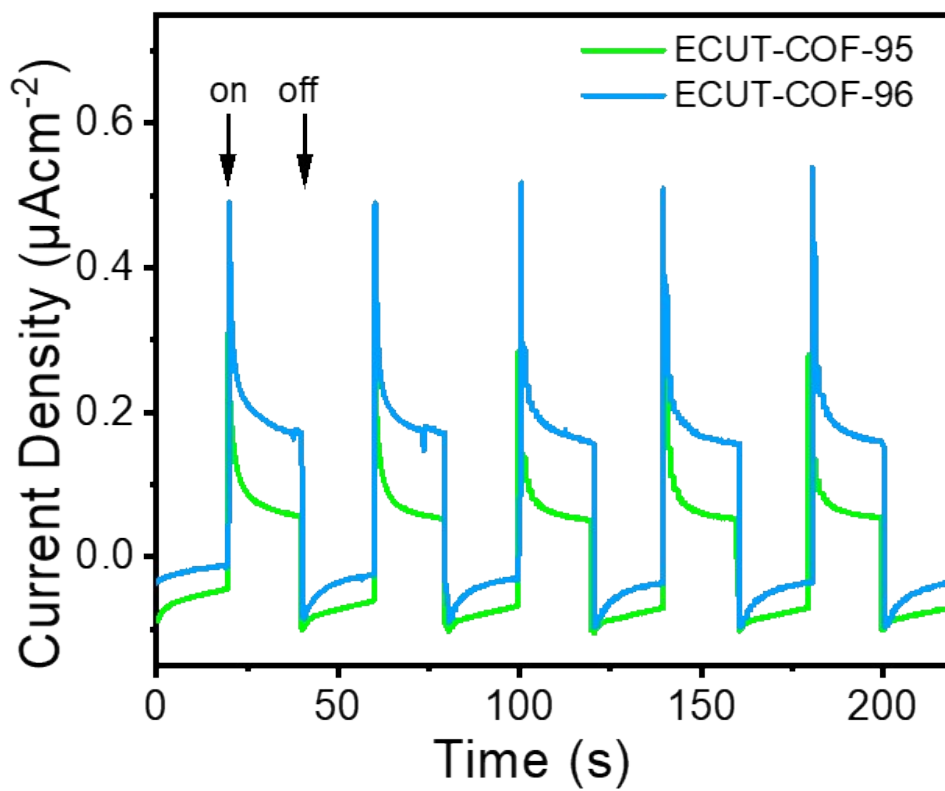


Fig. S7 Photocurrent response of ECUT-COF-95 and ECUT-COF-96.

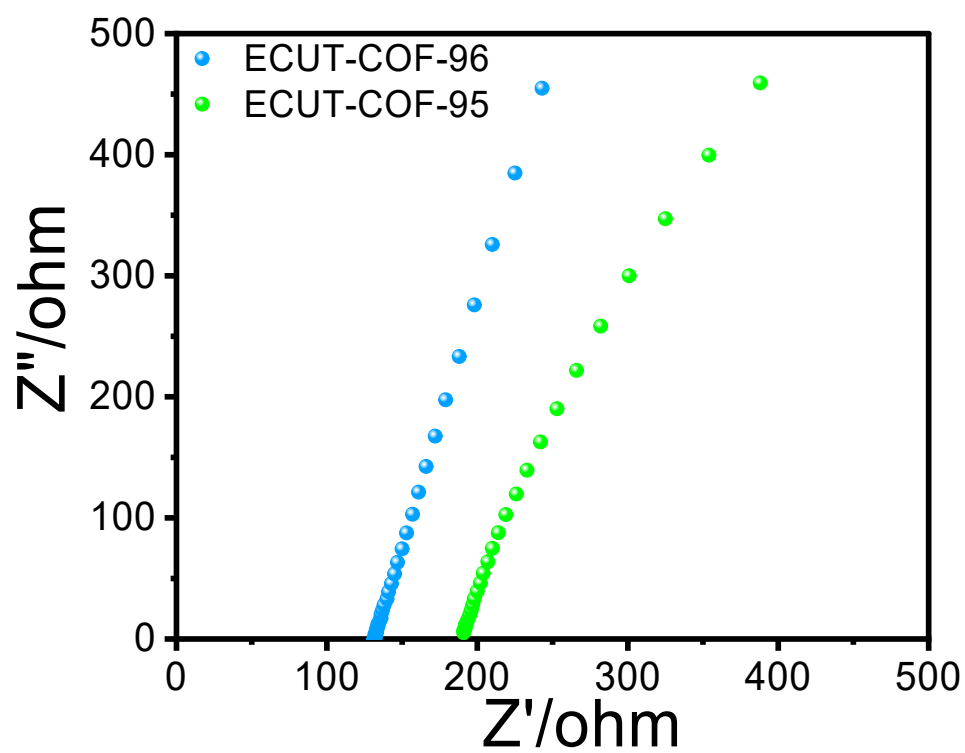


Fig. S8 electrochemical impedance (EIS) profiles of ECUT-MCOF-95 and ECUT-MCOF-96.

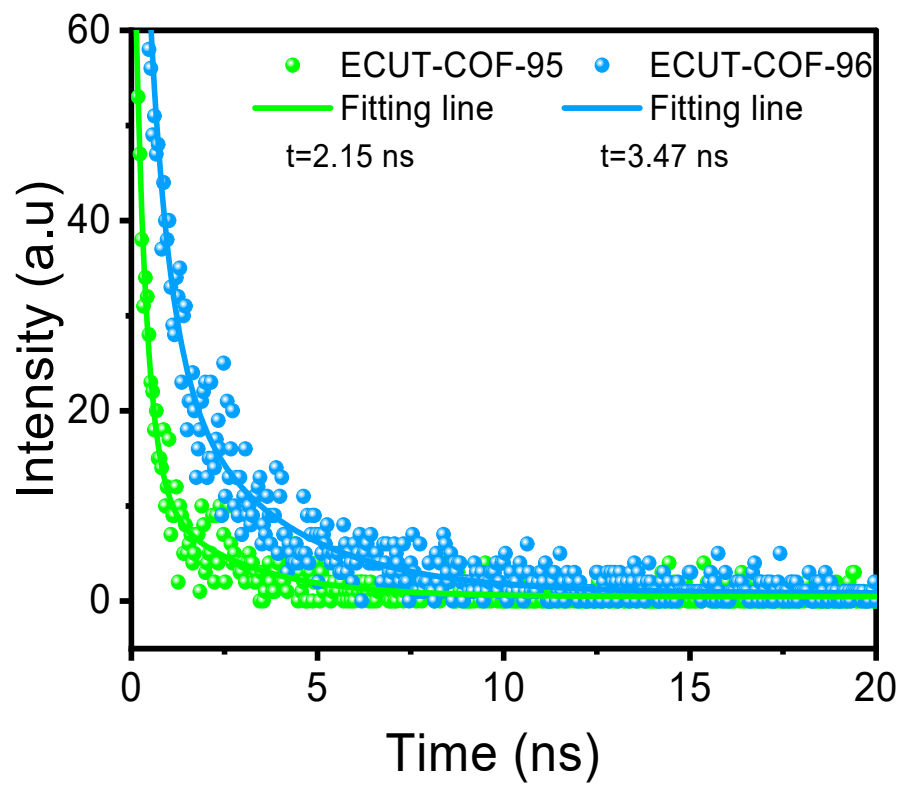


Fig. S9 TD-PL of ECUT-COF-95 and ECUT-COF-96.

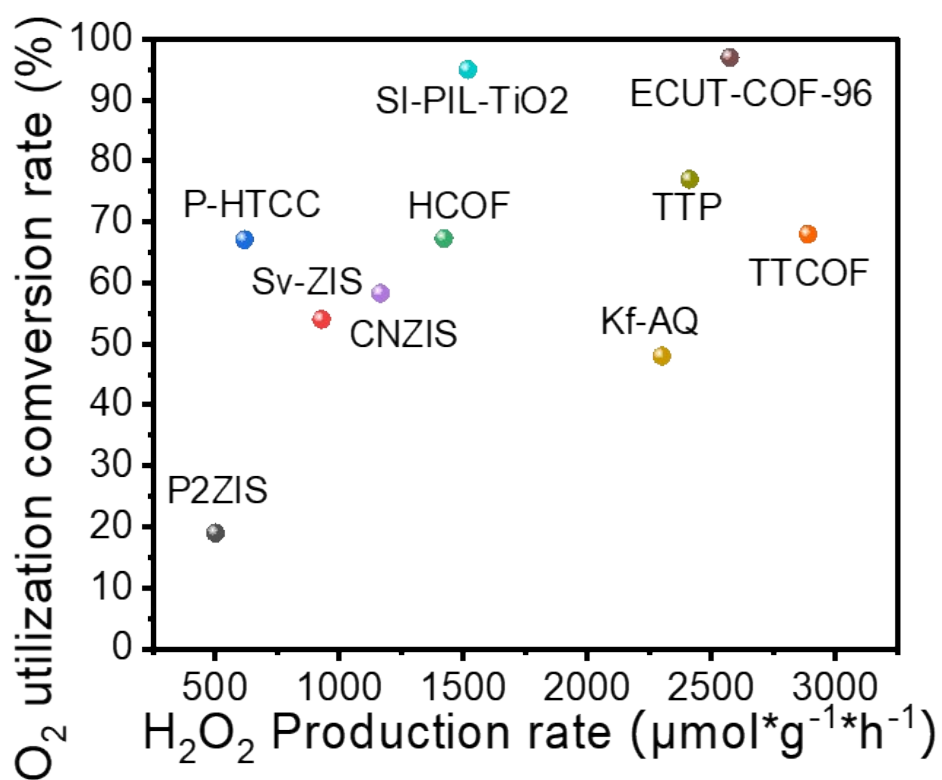


Fig. S10 Comparison of H_2O_2 production rates and O_2 utilisation and conversion rates.

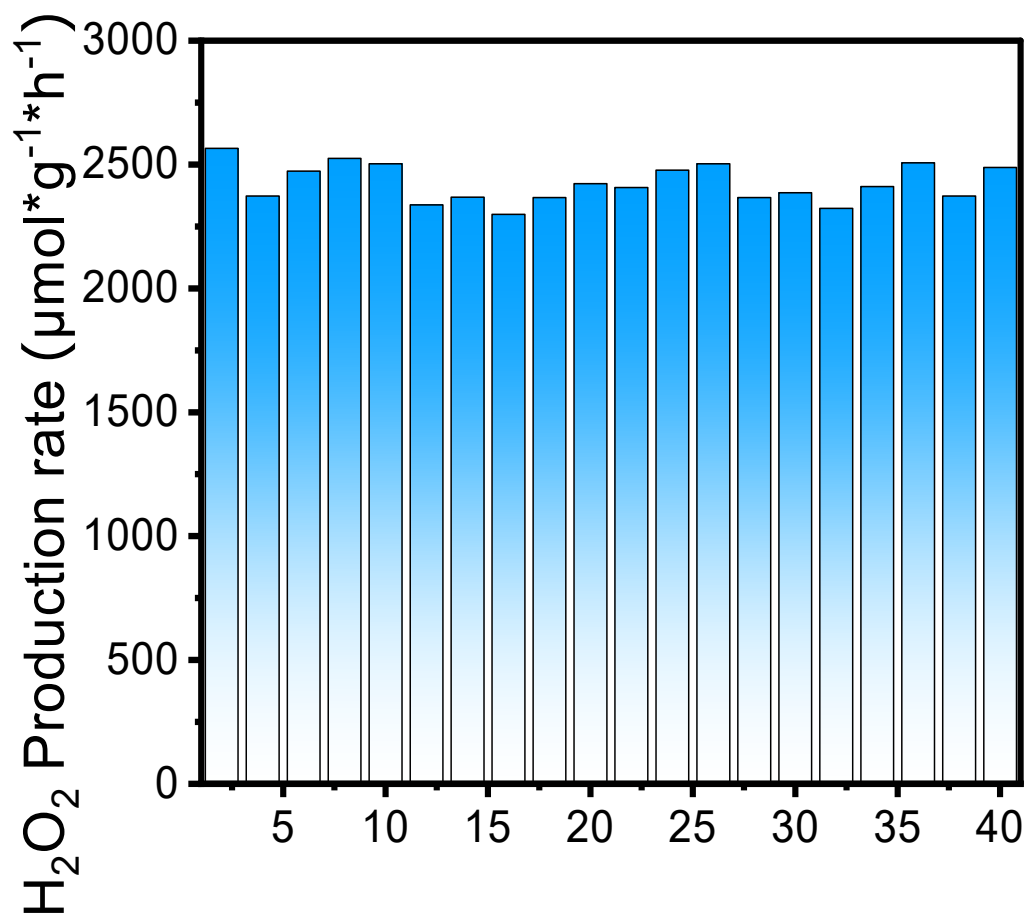


Fig. S11 ECUT-COF-96 40-hour cycling test.

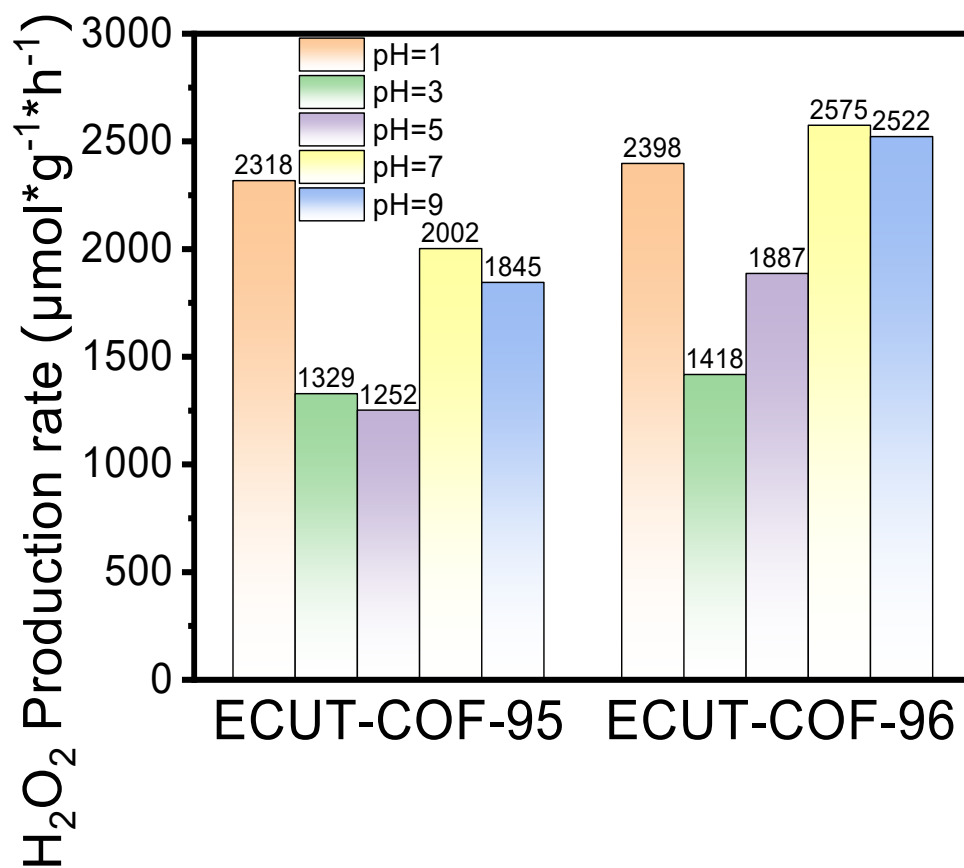


Fig. S12 H₂O₂ production under different pH conditions of ECUT-COF-95 and ECUT-COF-96.

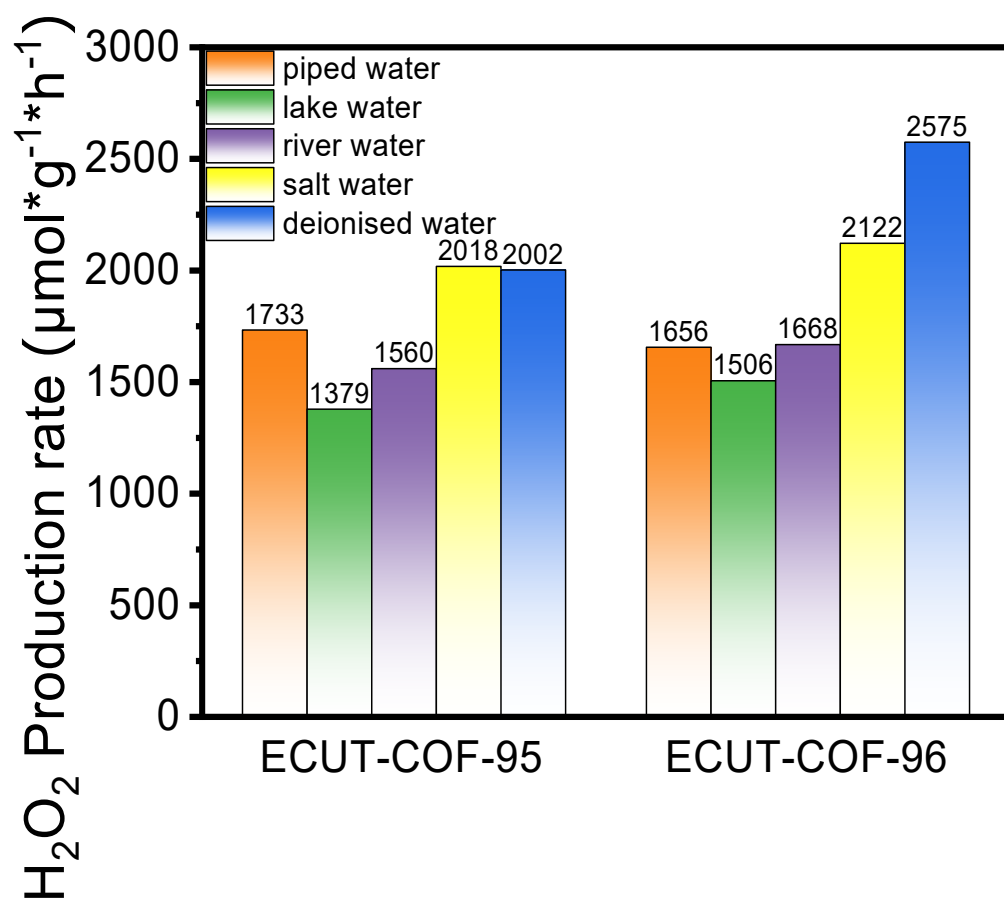


Fig. S13 H₂O₂ production in different waters of ECUT-COF-95 and ECUT-COF-96.

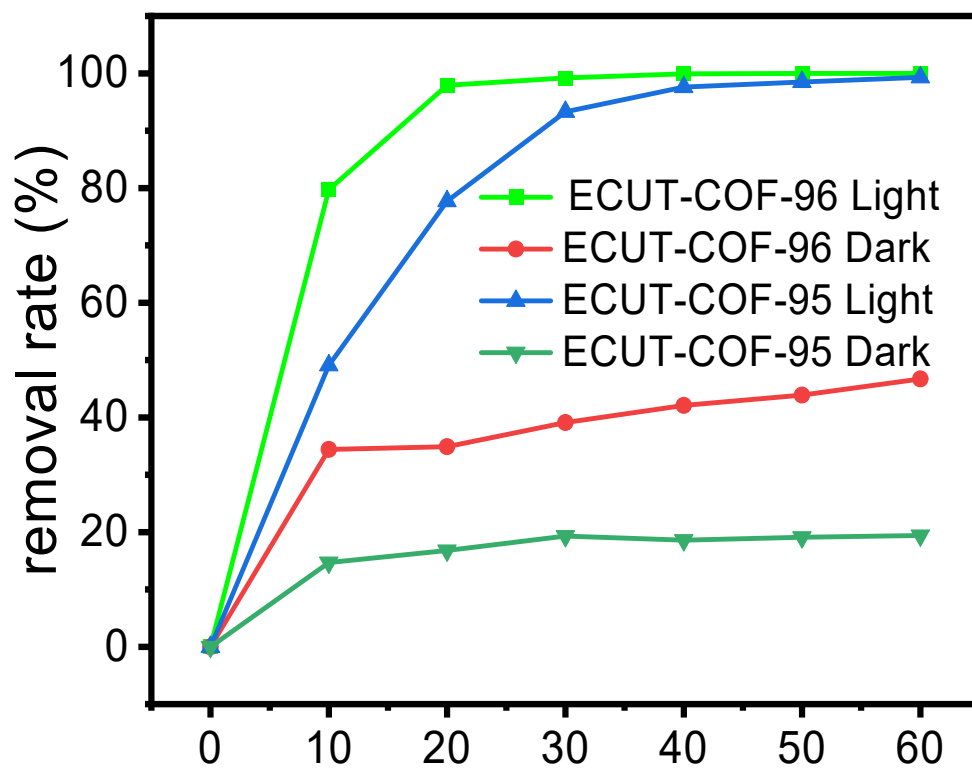


Fig. S14 Decomposition of Rhodamine B under different conditions.

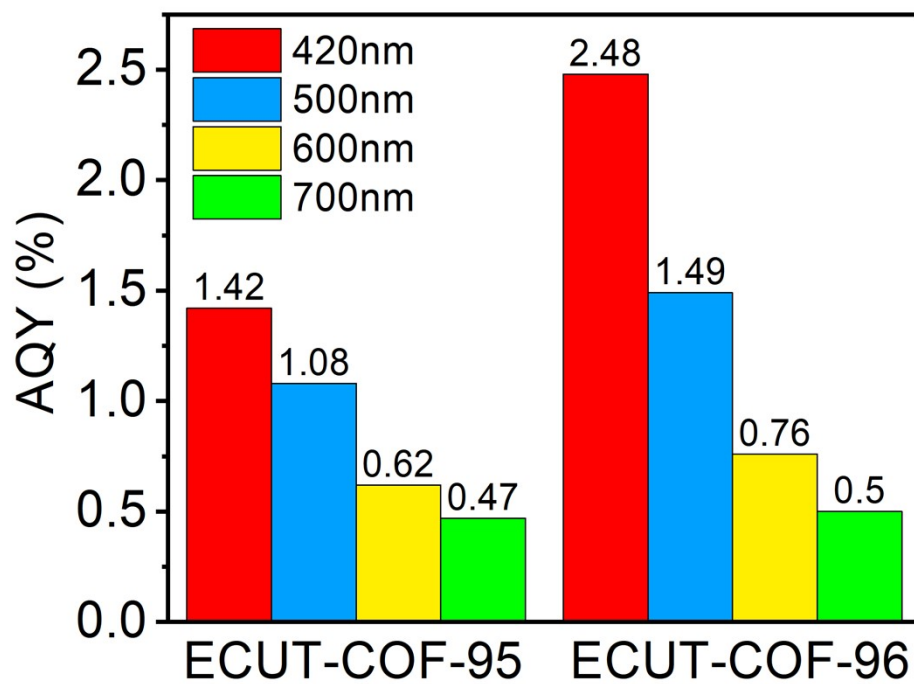


Fig. S15 AQY of ECUT-COF-95 and ECUT-COF-96 at different wavelengths.

Table S1. Calculated crystal data of ECUT-COF-95.

data_ECUT-COF-95							
_audit_creation_date		2024-07-09					
_audit_creation_method		'Materials Studio'					
_symmetry_space_group_name_H-M		'P-6'					
_symmetry_Int_Tables_number		174					
_symmetry_cell_setting		hexagonal					
loop_							
_symmetry_equiv_pos_as_xyz							
x,y,z							
-y,x-y,z							
-x+y,-x,z							
x,y,-z							
-y,x-y,-z							
-x+y,-x,-z							
_cell_length_a		22.8197					
_cell_length_b		22.8197					
_cell_length_c		3.5006					
_cell_angle_alpha		90.0000					
_cell_angle_beta		90.0000					
_cell_angle_gamma		120.0000					
loop_							
_atom_site_label							
_atom_site_type_symbol							
_atom_site_fract_x							
_atom_site_fract_y							
_atom_site_fract_z							
_atom_site_U_iso_or_equiv							
_atom_site_adp_type							
_atom_site_occupancy							
C1	C	0.96514	0.92958	0.50000	0.00000	Uiso	1.00
C2	C	0.03603	0.96491	0.50000	0.00000	Uiso	1.00
C3	C	0.07695	0.93120	0.50000	0.00000	Uiso	1.00
C4	C	0.05616	0.86468	0.50000	0.00000	Uiso	1.00
C5	C	0.08708	0.77353	0.50000	0.00000	Uiso	1.00
C6	C	0.13504	0.75256	0.50000	0.00000	Uiso	1.00
C7	C	0.20427	0.80051	0.50000	0.00000	Uiso	1.00
C8	C	0.22493	0.86936	0.50000	0.00000	Uiso	1.00

C9	C	0.17694	0.89030	0.50000	0.00000	Uiso	1.00
C10	C	0.10736	0.84265	0.50000	0.00000	Uiso	1.00
N11	N	0.25432	0.78037	0.50000	0.00000	Uiso	1.00
C12	C	0.23763	0.71110	0.50000	0.00000	Uiso	1.00
C13	C	0.35810	0.74023	0.50000	0.00000	Uiso	1.00
C14	C	0.28409	0.69139	0.50000	0.00000	Uiso	1.00
O15	O	0.37901	0.80105	0.50000	0.00000	Uiso	1.00
C16	C	0.18613	0.17125	0.50000	0.00000	Uiso	1.00
N17	N	0.22696	0.15530	0.50000	0.00000	Uiso	1.00
H18	H	0.93621	0.87189	0.50000	0.00000	Uiso	1.00
H19	H	0.13454	0.96278	0.50000	0.00000	Uiso	1.00
H20	H	0.03082	0.73438	0.50000	0.00000	Uiso	1.00
H21	H	0.11773	0.69625	0.50000	0.00000	Uiso	1.00
H22	H	0.28113	0.90870	0.50000	0.00000	Uiso	1.00
H23	H	0.19404	0.94657	0.50000	0.00000	Uiso	1.00
H24	H	0.30886	0.81926	0.50000	0.00000	Uiso	1.00
H25	H	0.18236	0.66915	0.50000	0.00000	Uiso	1.00

Table S2. Calculated crystal data of ECUT-COF-96.

data_ECUT-COF-96	
_audit_creation_date	2024-07-09
_audit_creation_method	'Materials Studio'
_symmetry_space_group_name_H-M	'P-6'
_symmetry_Int_Tables_number	174
_symmetry_cell_setting	hexagonal
loop_	
_symmetry_equiv_pos_as_xyz	
x,y,z	
-y,x-y,z	
-x+y,-x,z	
x,y,-z	
-y,x-y,-z	
-x+y,-x,-z	
_cell_length_a	22.6692
_cell_length_b	22.6692
_cell_length_c	3.5124

_cell_angle_alpha				90.0000			
_cell_angle_beta				90.0000			
_cell_angle_gamma				120.0000			
loop_							
_atom_site_label							
_atom_site_type_symbol							
_atom_site_fract_x							
_atom_site_fract_y							
_atom_site_fract_z							
_atom_site_U_iso_or_equiv							
_atom_site_adp_type							
_atom_site_occupancy							
C1	C	0.96358	0.92912	0.50000	0.00000	Uiso	1.00
C2	C	0.03492	0.96333	0.50000	0.00000	Uiso	1.00
C3	C	0.07473	0.92795	0.50000	0.00000	Uiso	1.00
C4	C	0.05240	0.86069	0.50000	0.00000	Uiso	1.00
C5	C	0.08083	0.76703	0.50000	0.00000	Uiso	1.00
C6	C	0.12797	0.74446	0.50000	0.00000	Uiso	1.00
C7	C	0.19810	0.79159	0.50000	0.00000	Uiso	1.00
C8	C	0.22024	0.86121	0.50000	0.00000	Uiso	1.00
C9	C	0.17306	0.88375	0.50000	0.00000	Uiso	1.00
C10	C	0.10273	0.83695	0.50000	0.00000	Uiso	1.00
N11	N	0.24773	0.77016	0.50000	0.00000	Uiso	1.00
C12	C	0.23174	0.70669	0.50000	0.00000	Uiso	1.00
C13	C	0.35360	0.73586	0.50000	0.00000	Uiso	1.00
C14	C	0.28413	0.68689	0.50000	0.00000	Uiso	1.00
C15	C	0.83019	0.01949	0.50000	0.00000	Uiso	1.00
N16	N	0.84748	0.07694	0.50000	0.00000	Uiso	1.00
H17	H	0.93337	0.87107	0.50000	0.00000	Uiso	1.00
H18	H	0.13277	0.95868	0.50000	0.00000	Uiso	1.00
H19	H	0.02393	0.72856	0.50000	0.00000	Uiso	1.00
H20	H	0.10929	0.68751	0.50000	0.00000	Uiso	1.00
H21	H	0.27707	0.89997	0.50000	0.00000	Uiso	1.00
H22	H	0.19146	0.94064	0.50000	0.00000	Uiso	1.00
H23	H	0.17591	0.66493	0.50000	0.00000	Uiso	1.00
H24	H	0.37027	0.79237	0.50000	0.00000	Uiso	1.00

Table S3. A comparison in sacrificial-agent-free H₂O₂ photosynthesis performance among reported materials and our cases.

Photocatalyst	H ₂ O ₂ production rate (μmol g ⁻¹ h ⁻¹) at O ₂	H ₂ O ₂ production rate (μmol g ⁻¹ h ⁻¹) at air	Light (nm)	O ₂ utilization(%)	AQY (%)		Reference
ECUT-COF-95	2075	2002	λ≥400	97	2.48	400	This work
ECUT-COF-96	2648	2575		97	1.42		
PyIm-COF	5850	4120	λ□420	70	3.7	420	Angew. Chem. Int. Ed. 2024, e202404563
TD-COF	4620	3364	400-700	73	\	\	Angew. Chem. Int. Ed. 2023, 62, e202309624.
TTCOF	4245	2890	400-700	68	\	\	
FS-OHOMe-COF	1100	500	λ≥420	45	9.6	420	Angew. Chem. Int. Ed. 2024, e202403926.
HCOF	2113.9	1421.6	λ≥420	67.3	3.41	550	Angew. Chem. Int. Ed. 2024, 63, e202408041.
FS-COFs	3904	3162	λ□400	81	6.21	420	Angew. Chem. Int. Ed. 2023, 62, e202305355
CuX-dptz	2685	1874	λ□400	70	0.4	400	Angew. Chem. Int. Ed. 2024, 63, e202316998.
TTP	3132	2412	λ≥420	77	7.61	420	Angew. Chem. Int. Ed. 2024, 63, e202317214.

SI-PIL-TiO ₂	1601	1518	$\lambda \geq 420$	95	\	\	Angew. Chem. Int. Ed. 2024, e202403926.
P ₂ ZIS	2652	500	$\lambda \geq 420$	19	\	\	Angew. Chem. Int. Ed. 2024, 63, e202317816.
Sv-ZIS	1706	928	$\lambda \square 400$	54	9.9	420	J. Am. Chem. Soc. 2023, 145, 27757-27766.